Quantum Terahertz Electrodynamics and Macroscopic Quantum Tunneling in Layered Superconductors

Sergey Savel'ev,[1,2] A. L. Rakhmanov,[1,2,3] and Franco Nori[1,4]

[1]Frontier Research System, The Institute of Physical and Chemical Research (RIKEN), Wako-shi, Saitama, 351-0198, Japan
[2]Department of Physics, Loughborough University, Loughborough LE11 3TU, United Kingdom
[3]Institute for Theoretical and Applied Electrodynamics RAS, 125412 Moscow, Russia
[4]Department of Physics and MCTP, University of Michigan, Ann Arbor, Michigan 48109-1040, USA

(Received 19 July 2006; published 14 February 2007)

We derive a quantum field theory of Josephson plasma waves (JPWs) in layered superconductors, which describes two types of interacting JPW bosonic quanta (one heavy and one lighter). We propose a mechanism of enhancement of macroscopic quantum tunneling (MQT) in stacks of intrinsic Josephson junctions. Because of the long-range interaction between junctions in layered superconductors, the calculated MQT escape rate Γ has a nonlinear dependence on the number of junctions in the stack. We show that the crossover temperature between quantum and thermal escape increases when increasing the number of junctions. This allows us to quantitatively describe striking recent experiments in $Bi_2Sr_2CaCu_2O_{8+\delta}$ stacks.

DOI: 10.1103/PhysRevLett.98.077002 PACS numbers: 74.72.Hs, 74.78.Fk

The recent surge of interest in stacks of intrinsic Josephson junctions is partly motivated by the desire to develop THz devices, including emitters [1,2], filters, detectors, and nonlinear devices [3]. Macroscopic quantum tunneling (MQT) has been, until recently, considered to be negligible in high-T_c superconductors due to the d-wave symmetry of the order parameter. Recent unexpected experimental evidence [4,5] of MQT in layered superconductors could open a new avenue for the applicability of stacks of Josephson junctions in quantum electronics [6]. This requires a quantum theory capable of quantitatively describing these remarkable experiments. In contrast to a *single* Josephson junction, *stacks* of *intrinsic* Josephson junctions are strongly coupled along the direction perpendicular to the layers because the thickness of these layers is of the order of a few nm, which is much smaller than the magnetic penetration length. This results in a profoundly nonlocal electrodynamics [2] that strongly affects quantum fluctuations in layered superconductors.

The two main results of this work are, first, the quantum electrodynamics of Josephson plasma waves (JPWs) and, second, the quantitative description of macroscopic quantum tunneling in stacks of Josephson junctions. Namely, using a general Lagrangian approach, we derive the theory of quantum JPWs, which describes *two interacting quantum fields*: a heavy JPW and a lighter one. We predict resonances in the amplitudes of quantum processes associated with the creation of pairs of JPW quanta. Using the general approach, we develop a quantitative theory of MQT in stacks of Josephson junctions. Our approach is based on the analysis of coupled sine-Gordon equations adequately describing the long-range interactions in $Bi_2Sr_2CaCu_2O_{8+\delta}$ stacks, in contrast to the phenomenological treatment [7] of capacitive coupled Josephson junctions. We derive the MQT escape rate Γ, which is strongly nonlinear with respect to the number of superconducting layers N, and changes to $\Gamma \propto N$ when N exceeds a certain critical value N_c. The thermoactivated escape rate Γ_T also increases in coupled junctions in comparison with decoupled ones. However, the crossover between quantum and thermal escape occurs at higher temperature for the coupled junctions. More important, our results are in good quantitative agreement with recent experiments [5].

Quantum theory for layered superconductors.—The electrodynamics of stacks of Josephson junctions can be described by the Lagrangian for the electromagnetic fields $\vec{E}$ and $\vec{H}$ interacting with matter: $\mathcal{L} = \frac{1}{c}\vec{j}\cdot\vec{A} + \frac{1}{8\pi}(\vec{E}^2 - \vec{H}^2)$, here without charge degrees of freedom. The current $\vec{j}$ consists of both the Josephson current across the layers (along the y axis, see top inset in Fig. 1(b)] and the London supercurrent along the layers (along the x axis); the vector potential is $\vec{A} = (A_x, A_y, 0)$. This Lagrangian can be rewritten as:

$$\mathcal{L} = \sum_n \int dx\left\{\frac{1}{2}\dot{\varphi}_n^2 + \frac{1}{2\gamma^2}\dot{p}_n^2 - \frac{1}{2}(\partial_x\varphi_n)^2 - \frac{1}{2}(\partial_y p_n)^2 - \frac{1}{2}p_n^2 + \cos\varphi_n + \frac{1}{2}(\partial_x p_n \partial_y \varphi_n + \partial_y p_n \partial_x \varphi_n)\right\}, \quad (1)$$

where $\varphi_n \equiv \chi_{n+1} - \chi_n - 2\pi s A_y^{(n)}/\Phi_0$ is the gauge-invariant interlayer phase difference, and $p_n \equiv (s/\lambda_{ab})\partial_x\chi_n - 2\pi\gamma s A_x^{(n)}/\Phi_0$ is the normalized superconducting momentum in the nth layer. Here, we introduce the phase χ_n of the order parameter, the interlayer distance s, the in-plane λ_{ab} and out-of-plane λ_c penetration depths, the anisotropy parameter $\gamma = \lambda_c/\lambda_{ab}$, and flux quantum Φ_0. The in-plane coordinate x is normalized by λ_c; the time t is normalized by $1/\omega_J$, where the plasma frequency is ω_J; also, $\partial_x = \partial/\partial x$, $\partial_y f_n = \lambda_{ab}(f_{n+1} - f_n)/s$, $\dot{} = \partial/\partial t$, and the z axis is pointed along the magnetic field. For simplicity, we now consider 2D fields with $\partial_z = 0$. The

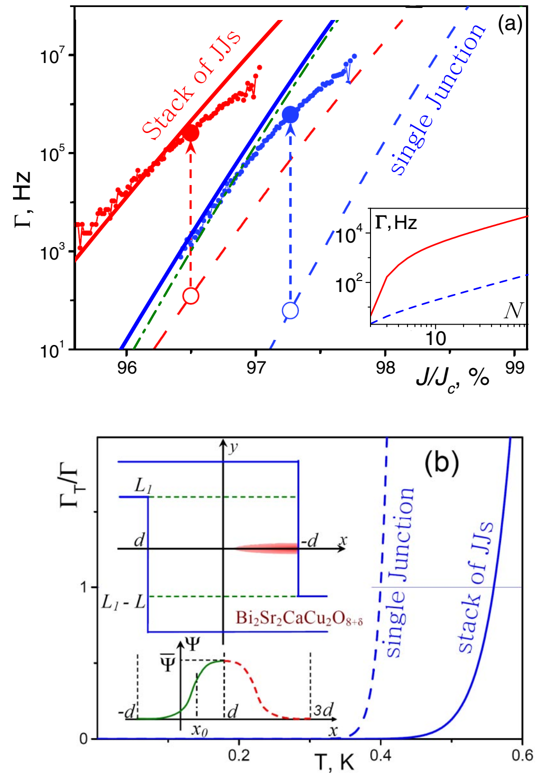

FIG. 1 (color online). (a) The MQT escape rate Γ versus dimensionless external current j. Red and blue points are the experimental data, from Ref. [5], for two different samples. Red and blue dashed lines are the curves $\Gamma_0(j)$ for these samples taken from [5]. Red and blue solid lines are the functions $\Gamma(j)$ calculated from our Eq. (7), while the green dashed-dotted line was obtained numerically from the nontruncated potential (5), using data from Table 1 of [5], for their samples US1 and US4. We use $s = 15$ Å, $\gamma = 300$ for blue and $\gamma = 150$ for red solid curves. The inset of (a) shows the dependence of the escape rate Γ versus the number of contacts N in the stack of Josephson junctions (JJs), using parameters for sample US4 of [5] at $j = 0.97$ (red solid line). The blue dashed line shows $N\Gamma_0$. (b) Our analytically obtained ratio Γ_T/Γ of thermal to quantum escape rates for the single-junction sample SJ1 (blue dashed) and the stack US4 (blue solid). Top inset in (b) shows the geometry studied, with a nucleating fluxon (red shadow). Bottom inset of (b) schematically shows a trial function (solid green line) and its periodic extension (red dashed line).

interaction between the p and φ fields occurs due to the $H^2 = (\partial_x A_y - \partial_y A_x)^2$ contribution to $\mathcal{L}$, resulting in the coupling term $\partial_x A_y \partial_y A_x$. Hereafter we ignore dissipation, which was shown [4,8] to be negligible. Varying the action $\mathcal{S} = \int dt \mathcal{L}$ produces

$$\begin{aligned} &\ddot{\varphi}_n - \partial_x^2 \varphi_n + \sin\varphi_n + \partial_x \partial_y p_n = 0, \\ &\frac{1}{\gamma^2} \ddot{p}_n - \partial_y^2 p_n + p_n + \partial_x \partial_y \varphi_n = 0, \end{aligned} \tag{2}$$

which reduces to the usual coupled sine-Gordon equations [9] for $\gamma^2 \gg 1$. Note that a Lagrangian approach for stacks of Josephson junctions can be formulated *only* for *two* interacting fields φ and p. This is because the vector potential has two components, A_x and A_y, in stacks of Josephson junctions, in contrast to 1D Josephson junctions where one component of the vector potential is enough.

Linearizing Eqs. (2) and substituting $p, \varphi \propto \exp(i\omega t + ik_x x + ik_y y)$ we derive a biquadratic equation, $(\omega^2 - k_x^2 - 1)(\omega^2/\gamma^2 - k_y^2 - 1) - k_x^2 k_y^2 = 0$, for the spectrum of the classical JPWs in the continuous limit (i.e., $k_y s \ll 1$) and $\gamma^2 \gg 1$. Here, k_x and k_y are the wave vectors (momenta in the quantum description, here, $\hbar = 1$) of the JPWs. This equation determines two branches, $\omega = \omega_a(\vec{k})$ and $\omega_b(\vec{k})$, of JPWs: $\omega_a(\vec{k}) = [1 + k_x^2/(1 + k_y^2)]^{1/2}$, $\omega_b(\vec{k}) = \gamma(k_y^2 + 1)^{1/2}$ up to $1/\gamma^2$. The a branch (b branch) describes Josephson plasmons propagating both along and perpendicular (only perpendicular) to the layers. In order to quantize the JPWs we use the Hamiltonian, $\mathcal{H} = \sum_n \int dx (\Pi_{\varphi_n} \varphi_n + \Pi_{p_n} p_n) - \mathcal{L}$, with the momenta Π_{φ_n} and Π_{p_n} of the φ_n and p_n fields, and require the standard commutation relations $[\varphi_{n'}(x'), \Pi_{\varphi_n}(x)] = i\delta(x - x')\delta_{n,n'}$, $[p_{n'}(x'), \Pi_{p_n}(x)] = i\delta(x - x')\delta_{n,n'}$ (all others commutators are zero), where δ is either a delta function or Kronecker symbol. Expanding $\cos\varphi_n = 1 - \varphi_n^2/2 + \varphi_n^4/24 - \ldots$, we can write $\mathcal{H} = \mathcal{H}_0 + \mathcal{H}_{\mathrm{an}}$, where we include terms up to φ_n^2 in $\mathcal{H}_0$, and the anharmonic terms in $\mathcal{H}_{\mathrm{an}}$. Diagonalizing $\mathcal{H}_0$, we obtain the Hamiltonian for the Bosonic free fields a and b: $\mathcal{H}_0 = \sum_{k_y} \int (dk_x/2\pi) \times \{\omega_a(\vec{k}) a^+ a + \omega_b(\vec{k}) b^+ b\}$. The original fields φ_n, p_n in Eq. (1) are related to the free Bosonic fields a and b by $\varphi \approx (a^+ + a)/(2\omega_a)^{1/2} - \mathcal{Z}(b^+ + b)/[\gamma(2\omega_b)^{1/2}]$ and $p \approx \mathcal{Z}(a^+ + a)/(2\omega_a)^{1/2} + \gamma(b^+ + b)/(2\omega_b)^{1/2}$, where $\mathcal{Z} = k_x k_y/(k_y^2 + 1)$. The spectra $\omega_a(\vec{k})$, $\omega_b(\vec{k})$ show that the "mass" of the a quantum equals one, and for the heavier b quasiparticle is γ.

The interaction between the a and b fields, including the self-interaction, occurs due to the *anharmonic* terms in $\mathcal{H}_{\mathrm{an}} \approx (-1/24)\sum_n \int dx \varphi_n^4 + \ldots$. In the leading order with respect to the bosonic field interactions, an a particle can create either $a + a$ or $a + b$ pairs. Using the spectra $\omega_{a,b}(\vec{k})$, one can conclude that the amplitudes of these processes have energy thresholds $\omega_a(\vec{k}_1) = 3$ or $\gamma + 2$ (similar to the $2mc^2$ rest energy threshold for $e^- + e^+$ pair creation in usual quantum electrodynamics). These result in resonances in the amplitudes of quantum processes (e.g., decay of a quanta).

Enhancement of macroscopic quantum tunneling.—Now we apply our theory to interpret very recent experiments [5] on MQT in $Bi_2Sr_2CaCu_2O_{8+\delta}$. To observe MQT, an external current J, close to the critical value J_c, was applied [5]. When tunneling occurs, the phase difference in a junction changes from 0 to 2π, which can be interpreted as the tunneling of a fluxon through the contact. This process can be safely described within a semiclassical approximation and we use the approach developed in Refs. [5,10] to calculate the escape rate

$\Gamma = \omega_P \sqrt{30B/\pi} \exp(-B)$ of a fluxon through the potential barrier. Here, ω_P is the oscillation frequency of a fluxon near the effective potential minimum, and $B = \int_{-\infty}^{\infty} d\tau \mathcal{L}(\tau = it) = 2\int_{\sigma_0}^{\sigma_1} ds[\varphi]\sqrt{2V[\varphi]}$ is described by the Lagrangian (1) with the classical fields determined by Eqs. (2). Integration should be performed in the functional space of φ between points $\sigma_{0,1}$ of zeros of the potential V along a trajectory $s[\varphi]$, which corresponds to the minimum of the effective action B (that is, the maximum of the escape rate). This is a complicated numerical problem, which can be replaced by integration over an appropriate set of trial functions. Below we will follow the latter approach.

Following the experimental setup [5], here we consider a stack of intrinsic Josephson junctions [see inset in Fig. 1(b)] having the size $L \gg s$ along the y direction; i.e., the total number of contacts $N = L/s \gg 1$, and the size in the x direction, $2d$, is smaller than the Josephson length, $\lambda_J = \gamma\sqrt{s\lambda_{ab}/2}$. In the limit $\gamma^2 \gg 1$, the equations for φ are reduced to standard coupled sine-Gordon equations [9], which in the continuum limit, $k_y s \ll 1$ and $y = ns/\lambda_{ab}$, become $(1 - \partial^2/\partial y^2)[\ddot{\varphi} + \sin\varphi] - \partial^2\varphi/\partial x^2 = 0$ with $\partial\varphi/\partial x = \pm jd/\lambda_c$ at $x = \pm d/\lambda_c$, where $j = J/J_c$.

We seek a solution φ of the form $\varphi = \psi(x, y, t) + \arcsin(j) + jx^2/2$, where the field ψ obeys

$$\left(1 - \frac{\partial^2}{\partial y^2}\right)[\ddot{\psi} - j(1 - \cos\psi) + \sqrt{1 - j^2}\sin\psi] - \frac{\partial^2\psi}{\partial x^2} = 0 \tag{3}$$

with boundary conditions $\partial\psi/\partial x = 0$ at $x = \pm d/\lambda_c$. In Eq. (3) inside square brackets we ignore the terms of the order of $d^2/\lambda_c^2 \sim 10^{-3}$ compared with $\sqrt{1 - j^2} \sim 0.1$.

We can linearize Eq. (3) in all junctions except one, where the fluxon tunnels. The linearized equation can be solved by using the Fourier transformation, $\psi = \sum_m \int \exp(-i\omega t)\exp(ik_{x,m}x)\psi_m(y, \omega)d\omega/2\pi$, where $k_{x,m} = \lambda_c \pi m/2d$. Here, in order to improve the convergence of the Fourier series, we expand the solution $\psi(x)$, initially defined for $-d < x < d$, periodically in $-\infty < x < \infty$, keeping continuous $\psi(x)$ and $\partial\psi(x)/\partial x$ [see inset in Fig. 1(b)]. Since in the experiment [5] the sample connects two bulk superconductors, we can choose the phase difference to be zero at the top ($y = L_1$) and bottom ($y = L_1 - L$) layers of the sample, and $y = 0$ corresponds to the position of the fluxon tunneling; see inset in Fig. 1(b). Using the continuity of $\psi(y)$ at $y = 0$, we derive the solution of the linearized equation in the form $\psi_m(y) = \psi_m(0)\sinh[q_m(L_1 - y)]/\sinh[q_m L_1]$, for $y > 0$, and $\psi_m(y) = \psi_m(0)\sinh[q_m(L - L_1 + y)]/\sinh[q_m(L - L_1)]$ for $y < 0$. Here, $q_m^2 = (k_{xm}^2 + \sqrt{1 - j^2} - \omega^2)/(\sqrt{1 - j^2} - \omega^2)$.

In the junction at $y = 0$, where the fluxon is tunneling, we cannot use the linearized equation. Instead we have $\ddot{\psi} - j(1 - \cos\psi) + \sqrt{1 - j^2}\sin\psi = \delta J_y/J_c$, where δJ_y is the current flowing through the junction at $y = 0$ due to its coupling with all the other junctions. In order to derive δJ_y, we use the Maxwell equations $J_x = -(c/4\pi\lambda_{ab})\partial H/\partial y$, $\delta J_y = (c/4\pi\lambda_c)\partial H/\partial x$, and the standard relation [11], $\partial\psi(y=0)/\partial x = 8\pi^2\lambda_{ab}^2\lambda_c[J_x(y = +0) - J_x(y = -0)]/c\Phi_0$, between the phase difference and the in-plane current; H is the magnetic field. Following the approach described in Ref. [2] we obtain $\delta J_y/J_c = \lambda_J^2/(\lambda_c^2) \times \int_{-\infty}^{\infty} d\omega/(2\pi)e^{-i\omega t}\sum_{m=-\infty}^{\infty} k_{x,m}^2 \mathcal{G}_m e^{ik_{xm}x}\psi_m(\omega)$, where $\mathcal{G}_m = \sinh(q_m L_1)\sinh[q_m(L_1 - L)]/q_m \sinh(q_m L)$. Neglecting contributions to the tunneling process arising from higher frequencies, $\omega \geq \omega_J(1 - j^2)^{1/4}$, and performing a reverse Fourier transform, $\psi_m = (\lambda_c/2d)\int\psi(x) \times \exp(-ik_{xm}x)dx$, we derive

$$\frac{\delta J_y}{J_c} = \frac{\lambda_J^2}{2d\lambda_c}\sum_{m=0}^{\infty} k_{x,m}^2 \mathcal{G}_m \int_{-d/\lambda_c}^{d/\lambda_c} dx'\psi(x')\cos k_{xm}(x - x'). \tag{4}$$

Next, we construct an effective potential $V[\psi]$ choosing a proper trial function ψ. The tunneling fluxon can be described as a smeared steplike function [see inset in Fig. 1(b)], which can be parameterized by the fluxon position x_0 and the height $\bar{\psi}$ of the step in ψ. We assume that $\ddot{\bar{\psi}} \gg \ddot{x}_0$. This quite natural assumption agrees well with recent numerical simulations [12]. Indeed, the fluxon starts penetrating at the sample edge where the induced current δJ_y suppresses the barrier. Staying in this position, the amplitude of ψ increases, overcoming the barrier. As soon as the barrier is overcome, the fluxon moves classically towards the other sample edge. Integrating $\psi(y = 0)$ over x, we derive for $\bar{\psi}$ the equation: $d^2\bar{\psi}/dt^2 = -\partial V/\partial\bar{\psi}$. Here the effective potential $V(\bar{\psi})$ can be written as

$$V(\bar{\psi}) = j(\sin\bar{\psi} - \bar{\psi}) - \sqrt{1 - j^2}\left(\cos\bar{\psi} - 1 + \frac{g_n\bar{\psi}^2}{2}\right),$$
$$g_n(j) = -\frac{\gamma s}{2x_0 d}\sum_{m=0}^{m_{\max}} \frac{\mathcal{G}_{2m+1}[1 - \cos(k_{x2m+1}x_0)]}{\sqrt{1 - j^2}}, \tag{5}$$

where $n = L_1\lambda_{ab}/s$ labels the contact through which the fluxon tunnels and $2m_{\max} + 1 < d/2\gamma s$. Harmonics with $m > m_{\max}$ oscillate fast on a scale of the fluxon core, of about $\gamma s < d$, producing a small correction to the effective potential. Note that the vortex core size of about $\gamma s \ll \lambda_J$ due to nonlocal effects [2]. For the samples used in the experiment [5] we find $m_{\max} \approx 1$. Keeping only the two first harmonics and optimizing the form of the tunneling fluxon with respect to x_0 we derive

$$g_n(j) \approx 0.23Q\frac{\sinh(Qn)\sinh[Q(N - n)]}{\sinh(QN)}, \tag{6}$$

and $Q(j) = \pi\gamma s/2d(1 - j^2)^{1/4}$. Note that this optimization reduces to finding the maximum of $(1 - \cos k_{x1}x_0)/k_{x1}x_0$. The obtained optimal position x_0 of the tunneling vortex, which is about $0.4d$ from the sample edge, is close to that found numerically [12] when optimizing the real shape of the fluxon.

Following a semiclassical approach [10] we calculate the effective action $B = 2\int_0^{\psi_1}[2V(\bar{\psi})]^{1/2}d\bar{\psi}$, where $V(\bar{\psi}_1) = 0$. This can be done either numerically (see green dashed-dotted curve in Fig. 1) or analytically. For an applied current J close to J_c, we can expand both $\cos\bar{\psi}$ and $\sin\bar{\psi}$ and obtain $V(\bar{\psi}) = -\bar{\psi}^2(\bar{\psi} - \psi_1)/6$, where $\psi_1(j) = 3\sqrt{1-j^2}[1 - g_n(j)]$. Taking into account that the fluxon can tunnel through any junction of the stack, we derive an analytical expression for $\Gamma(j)$ (in dimensional units)

$$\frac{\Gamma(j)}{\Gamma_0(j)} = \sum_{n=0}^{N}(1-g_n)^{5/4}\exp\left\{-\frac{36U_0}{5\hbar\omega_P}[(1-g_n)^{5/2}-1]\right\}, \tag{7}$$

where the summation is taken over all N contacts. Here, the effective Josephson frequency is $\omega_P(j) = \omega_J(1-j^2)^{1/4}$, the height of the potential barrier $U_0(j) = 2E_J(1-j^2)^{3/2}/3$, the Josephson energy $E_J = \Phi_0 J_c/2\pi c$, and the escape rate $\Gamma_0(j)$ for a single Josephson junction (see, e.g., [5]) is given by $\Gamma_0(j) = [216\omega_P(j)U_0(j)/\pi\hbar]^{1/2} \times \exp[-36U_0(j)/5\hbar\omega_P(j)]$. The red and blue solid lines in Fig. 1(a) show $\Gamma(j)$, which describe well the experimental results in [5]. Some deviation between the experimental data and the theoretical prediction at high currents is due to a significant lowering of the potential barrier resulting in a decrease of the accuracy of the semiclassical approximation. The dependence of Γ on the number N of junctions is nonlinear, more complicated than N^2 dependence, due to the long-range interaction between different junctions, described by the last term in the expression (5) for the effective potential. This nonlinearity is strong for relatively small $N \lesssim N_c = d/\gamma L$, and the escape rate Γ becomes proportional to N when the thickness L of the stack exceeds the effective interaction length d/γ. However, for the parameters used in the experiment [5] the value $\Gamma(j)$ obtained here nicely mimics the N^2 dependence measured in the experiment. The predicted strongly nonlinear dependence of the escape rate on N [see inset of Fig. 1(a)] could be an experimentally realizable test of our model.

The thermoactivated escape rate, $\Gamma_T(j) = [\omega_P(j)/2\pi]\sum_n \exp\{-E_J \max[V_n(\bar{\psi})]/k_B T\}$ with Boltzmann constant k_B, also increases due to the mutual interaction between junctions in the stack. In our analytical approach we have $\max(V_n) = 2\psi_1^3(n)/81$. The ratio, $r(T) = \Gamma_T/\Gamma$, between thermal and quantum escape rates is shown in Fig. 1(b) as a function of temperature for the single junction SJ1 and the stack US4 used in Ref. [5]. The thermoactivated escape starts to play a significant role ($r(T) > 1$) at $T \approx 0.6$ K for the stack and at $T \approx 0.4$ K for the single junction, in agreement with experiments [5].

Note that a more elaborated theory of MQT in layered superconductors should include the effects of intrinsic dissipation and interaction with the environment (shunting impedance). As it was shown in Ref. [8], the intrinsic dissipation renormalizes Γ by a factor of about 0.9 for the considered case of the c axis junctions. Thus, the main source of dissipation for stacks of intrinsic Josephson junctions is the shunting impedance, which can be ignored if the Josephson inductance, $2e/\hbar J_c$, is smaller than the inductance of the shunting circuit. It is evident that such a condition was satisfied for experiment [5] since the escape rate for the single-junction sample SJ3 is well described by $\Gamma_0(j)$, where dissipation is ignored.

Very different types of MQT models in stacks of Josephson junctions, with no quantitative comparison with experimental data, are also studied in [7]. Here we consider the inductive coupling among layers, which is known to be strong, instead of the capacitive coupling among layers used in [7], which is known to be weak. Moreover, theory [7] considers a model for photon-assisted MQT tunneling instead of the current-biased tunneling observed in Ref. [5].

Conclusions.—We consider quantum excitations in stacks of junctions described by two Bosonic fields, one lighter a and the other heavier b. We also derive the interaction of these quantum fields and predict resonances when either $a + a$ or $a + b$ pairs are produced. We suggest a semiclassical theory of the fluxon quantum tunneling in stacks of intrinsic Josephson junctions, which is in good agreement with recent remarkable experimental observations. The obtained results might be potentially useful for future designs of quantum devices.

We acknowledge M. Machida, T. Koyama, and S. Kawabata for stimulating discussions and partial support from the NSA, LPS, ARO, NSF Grant No. EIA-0130383, JSPS-RFBR No. 06-02-91200, RFBR No. 06-02-16691, MEXT Grant-in-Aid No. 18740224, and the EPSRC via No. EP/D072581/1.

[1] R. Kleiner *et al.*, Phys. Rev. Lett. **68**, 2394 (1992); G. Hechtfischer *et al.*, *ibid.* **79**, 1365 (1997); E. Goldobin *et al.*, Phys. Rev. B **57**, 130 (1998); J. Zitzmann *et al.*, *ibid.* **66**, 064527 (2002); M. Tachiki *et al.*, *ibid.* **71**, 134515 (2005); A. A. Abdumalikov *et al.*, *ibid.* **72**, 144526 (2005).
[2] S. Savel'ev *et al.*, Phys. Rev. B **72**, 144515 (2005).
[3] S. Savel'ev *et al.*, Phys. Rev. Lett. **94**, 157004 (2005); **95**, 187002 (2005); Nature Phys. **2**, 521 (2006); Phys. Rev. B **74**, 184512 (2006); V. A. Yampol'skii *et al.*, Phys. Rev. B **75**, 014527 (2007).
[4] K. Inomata *et al.*, Phys. Rev. Lett. **95**, 107005 (2005); T. Bauch *et al.*, *ibid.* **94**, 087003 (2005); T. Bauch *et al.*, Science **311**, 57 (2006).
[5] X. Y. Jin *et al.*, Phys. Rev. Lett. **96**, 177003 (2006).
[6] J. Q. You and F. Nori, Phys. Today **58**, No. 11, 42 (2005); A. J. Berkley *et al.*, Science **300**, 1548 (2003).
[7] M. Machida and T. Koyama, cond-mat/0605404.
[8] S. Kawabata *et al.*, Phys. Rev. B **70**, 132505 (2004); **72**, 052506 (2005).
[9] L. N. Bulaevskii *et al.*, Phys. Rev. B **50**, 12 831 (1994).
[10] S. Coleman, Phys. Rev. D **15**, 2929 (1977).
[11] A. Gurevich, Phys. Rev. B **46**, 3187 (1992).
[12] A. O. Sboychakov (unpublished).